PEP-NOTE--381

DE90 008580

Tune Shift and Betatron Modulations due to Insertion Devices in SPEAR*

W.J. Corbett
Storage Rings Division
Stanford Linear Accelerator Center
Stanford University, Stanford, California 94309

Abstract

SPEAR will soon operate as a dedicated synchrotron radiation source with up to 5 beamlines fed from insertion devices. These magnets introduce additional focusing forces into the storage ring lattice which increase the vertical betatron tune and modulate the beam envelope in the vertical plane. The lattice simulation code 'GEMINI' is used to evaluate the tune shifts and estimate the degree of betatron modulation as each magnetic insertion device is brought up to full power. A program is recommended to correct the tunes with the FODO cell quadrupoles.

*Work supported by U.S. Department of Energy Contract DE-AC03-76SF00515

I. Introduction

Figure 1 shows a plot of the vertical betatron function and horizontal dispersion function in a standard SPEAR lattice with no insertions active. The locations of the 5 SSRL insertion devices are denoted by {I4,I5,I6,I7,I10} in this plot. For simplicity, these devices will be referred to as wigglers, regardless of their output spectra. Note that the wigglers are located in straight sections where the vertical betatron function has local minima and the horizontal dispersion function reaches local maxima. The numerology of the wigglers correspond to the standard SSRL beamline nomenclature for SPEAR[1], and their characteristics are listed in Table 1.

Element	Type	Beamline	Period (cm)	#Period	Field Strength
Wiggler [I4]	Electro-magnet	4	45cm	4	0-18kG
Wig./Und. [I6]	Perm. Mag.	6	7cm	27	0-13kG
Wiggler [I7]	Electro-magnet	4	45cm	4	0-18kG
Wig./Und. [I10]	Nd-Fe-B +EM Hybrid	10	12.85cm	15	0-14.5kG
Undulator	SmCo Perm. Mag.	5	18.3cm 12.2cm 7.6cm 6.1cm	10 15 24 30	0-15kG

Table 1: SSRL insertion devices in SPEAR (1989).

The magnet lattice is taken directly from SPEAR (9/28/87) with a small adjustments made to the quadrupole strengths to eliminate the peak-to-peak betatron modulation around the ring. Although the horizontal dispersion shows some beating, studies show that trying to improve the configuration results in unacceptable vertical betatron amplitudes near the Q2 quadrupoles. The basic machine operating parameters are:

$E_0 = 3\text{GeV}$ $(B\rho = 10\ \text{T-m})$ $\nu_x = 5.2734$ $\nu_y = 5.1076.$

And the quadrupole and sextupole focussing strengths are

Q3: k=-0.917820768037 m^{-2}	L=1.0000m	SDA : k2=-4.89704 m^{-3}	
Q2: k=0.3915455527850	L=1.3427	SF : k2= 7.92276	
Q1: k=-0.240660980525	L=0.5183	SDB : k2=-4.68611	
QFA:k=0.5746900485390	L=0.5183	L_{sext} = 0.1000m	
QDA:k=-0.558139700304	L=0.5183		
QFB:k=0.2778567196980	L=0.5183		
QF: k=0.2931844261380	L=0.5183		
QDH:k=-0.526836403609	L=0.2591		
QFS: k=0.2974200000000	L=0.5183		

Table 2: SPEAR machine parameters

where $k=k_x=\frac{1}{B\rho}\cdot\frac{dB_y}{dx}$ (m^{-2}) is the focusing strength of the quadrupoles, L is the magnetic length of the quadrupoles and sextupoles, and $k2 = k2_x=\frac{1}{B\rho}\cdot\frac{dB_y^2}{dx^2}$ (m^{-3}).

As the SSRL wiggler devices are introduced into the lattice, they act as additional vertical focusing elements with a quadrupole focusing strength proportional to the square of the peak field strength, B_0^2. The additional focusing forces increase the vertical betatron tune, and generate beta-function perturbations which propagate around the ring. The net effect of the perturbation is particularly complicated in SPEAR since the mini-β insertion quadrupoles are strong and the magnet lattice is configured to match the HEP interaction points to the arcs.

The normal set-up procedure on SPEAR for SSRL operations is to first establish an orbit at full energy with no insertions active and requiring a minimum of orbit corrections. This is followed by exciting the electromagnet wigglers {I4, I7} in tandem while maintaining stable beam conditions, and finally, sequentially turning on insertions I5, I6, I10. For this study, the 3GeV beam energy is held constant.

In this memo, the linear tune shift induced by the wiggler/undulators and the vertical betatron modulation, $\Delta\beta/\beta$ are first estimated analytically. These results are compared with the lattice simulation code 'GEMINI'[2] which contains a model for magnetic wiggler/undulators[3]. The wigglers are first ramped up to maximum field strength individually, and then ramped in sequence to simulate the operating conditions in SPEAR. By correcting the vertical tune at each step, a plot of requisite change in the quadrupole strengths (QF and QDH in the main FODO cells) is obtained. These results provide a guideline for the machine operator interested in restoring the betatron tunes. Finally, the

modulations in the vertical betatron function, $\frac{\Delta\beta(s)}{\beta(s)}$ produced in SPEAR as the wigglers are brought on line are discussed.

II. Linear Tune Shift Estimate

We proceed by first estimating the equivalent quadrupole focusing of the wigglers. The focusing shifts the tunes and alters the betatron function around the ring. These calculations will be compared to the numerical results below.

To begin, the magnetic field structure in the current-free region of the wiggler gap can be expressed in terms of a magnetic potential, Φ_M. By separation of variables, we have,

$$\nabla^2\Phi_M = \frac{d^2\Phi_M}{dy^2} + \frac{d^2\Phi_M}{dz^2} \qquad 2.1$$

where $\frac{d}{dx} = 0$, that is, the gap height is assumed to be much smaller than the wiggler channel width. By separating transverse and longitudinal variables, $\Phi_M(y,z) = Y(y)\cdot Z(z)$,

$$\nabla^2\Phi_M = \frac{Y''}{Y} + \frac{Z''}{Z}$$

$$\frac{Y''}{Y} = -\frac{Z''}{Z} = \lambda^2$$

$$Y = A\cos ky + B\sin ky$$
$$Z = A'\cosh kz + B'\sinh kz \qquad 2.2$$

where $k=\frac{2\pi}{\lambda}$ is the wavenumber of the wiggler field. The effects of higher harmonics of the wavenumber can be linearly superimposed. Solving for the field, $\underline{B} = -\underline{\nabla}\Phi_M$, and applying boundary conditions appropriate to the wiggler structure we have:

$$B_y = B_0\cosh ky \cos kz$$

$$B_z = B_0\sinh ky \sin kz\ . \qquad 2.3$$

Now the horizontal trajectory of an electron bunch passing through the wiggler is deflected ('wiggled') by the vertical component B_y by an angle[4]

$$\theta(z) = \frac{e}{cp_0}\int_0^z B_z dz = \frac{e}{cp_0} B_0 \cosh ky \int_0^z \cos kz\, dz$$

$$\theta(z) = -\frac{e}{cp_0} B_0 \cosh ky \frac{\sin kz}{k}, \qquad 2.4$$

which causes the bunch to see a transverse component of the longitudinal wiggler field (B_z) of magnitude $B_\perp = B_z \sin\theta(z) \sim B_z \theta(z)$ for small angles θ. Substituting for B_z and θ,

$$B_\perp = -\frac{e}{cp_0} (B_0 \sin kz)^2 \left[\frac{\sinh ky \cosh ky}{k}\right].$$

Expanding the hyperbolic functions

$$\cosh ky = \sum_{n=0}^{\infty} \frac{(ky)^{2n}}{2n!}, \quad \sinh ky = \sum_{n=0}^{\infty} \frac{(ky)^{2n+1}}{(2n+1)!}$$

we have $$B_\perp = -\frac{e}{cp_0} (B_0 \sin kz)^2 \left[y + \frac{2}{3} k^2 y^3 + \cdots \right]. \qquad 2.5$$

The wiggler focusing is derived from the Lorentz force $v_z \times B_\perp$ and is quadradic in B_0. The force contains a linear (quadrupole) component proportional to displacement in y. Integrating the focusing strength over one half period (pole) of the wiggler magnet,

$$k_{wig} l = \frac{1}{B\rho} \cdot -\frac{e}{cp_0} B_0^2 \int_0^z \sin^2 kz dz$$

$$k_{wig} l = \left[\frac{eB_0}{cp_0}\right]^2 \frac{\lambda}{4} = -\frac{1}{4} \frac{\lambda}{\rho_o^2}, \qquad 2.6$$

where ρ_o^2 is the inverse bending radius at the center of the wiggler pole where the field reaches the maximum value B_0. The minus sign implies focusing in the vertical plane. An 'N'-period wiggler therefore has an equivalent quadrupole strength of

$$k_{wig} l = -\frac{N}{\rho_0^2} \frac{\lambda}{2}. \qquad 2.7$$

This expression[4] gives the equivalent thin-lens quadrupole focusing for a wiggler. In practice, the beam envelope and betatron phase advance through wiggler gap, and numerical integration is required for a more complete solution.

The perturbation to the tune shift due to a δ-function focusing kick at the wiggler is approximately

$$\Delta\nu_y = -\frac{1}{4\pi} \int \beta_y(s)\, kl \cdot \delta(s - s_{wig})\, ds = -\frac{1}{4\pi} \beta_{y,wig}\, k_{wig} l. \qquad 2.8$$

For the wigglers in Table 1, the linear tune shifts at full magnetic field strength for a 3GeV beam are

Element	$k_{wig}l$	Vertical Beta (m)	Tune Shift : $\Delta\nu_y$	$\Delta\beta/\beta$
I4	-0.0292	4.28	0.0099	5.2%
I7	-0.0292	4.28	0.0099	1.1%
I5**	-0.0206	4.71	0.0077	4.5%
I6	-0.0160	4.29	0.0055	-2.7%
I10	-0.0202	4.33	0.0070	-1.8%

**product $N\lambda$ assumed constant for all 4 configurations on I5.

Table 3: Estimated tune shifts and betatron modulation.

The betatron modulation $\frac{\Delta\beta}{\beta}$ tabulated in the last column of this table is evaluated using the expression

$$\frac{\Delta\beta_1}{\beta_1} = -\frac{1}{2\sin 2\pi\nu_y} \Sigma\, k_{wig} l \beta_{wig} \cos 2\nu_y(\pi - |\Phi_{wig} - \Phi_1|) \qquad 2.9$$

near beamline 4 at a position s=70m from the West Interaction Point (MII) where numerical plots of $\frac{\Delta\beta}{\beta}$ indicate the perturbations are large. $\Phi = 2\pi \int_0^s \frac{ds}{\nu_y \beta}$ is the phase advance (normalized to the tune) around the accelerator. The linear approximations for the perturbed betatron motion and tune shift listed in Table 3 agree reasonably well with the more precise numerical results obtained below. In the approximations made here, the horizontal tune shift is negligible.

III. Numerical Results

In this section, the SPEAR lattice with 5 SSRL insertion devices is analyzed with the lattice simulation code 'GEMINI'[2]. which incorporates wiggler elements based on the Halbach model with up to eight harmonics[3]. Numerical solutions are generated in GEMINI utilizing a 4th-order symplectic integrator technique[2]. For this study, GEMINI was instructed to perform the following calculations:

(1) Ramp insertions separately, monitor tune shifts.
(2) Ramp insertions sequentially, monitor tune shifts.
(3) Ramp insertions sequentially, correct tune shift, then
  (a) Record quadrupole strength in FODO cells.
  (b) Plot $\frac{\Delta\beta}{\beta}$ at B_{max} for each device.

Figure 2 shows a plot of the vertical tune shift in SPEAR calculated for the case where each insertion device is progressively excited independently. The tune shift for beamlines 4 and 7 are combined since they are normally operated in parallel. As per Eqn. 2.8, ν_y increases quadradically with pole strength B_0. Comparing with Table 3, we find good agreement with the linear tune shift estimate in each case.

For the case where the wigglers are excited serially, Fig. 3 shows a plot of the vertical tune increase. Beamlines 4 and 7 are again operated in parallel. The total tune shift expected with all 5 wigglers operating at peak field is on the order of 0.04. This increase can push the tune across synchrobetatron resonance lines on the operating diagram for SPEAR.

To correct the tunes, the quadrupole families QF and QDH are used. In the simulation, we fit the tunes following each 1kG increment of field strength as the wigglers are ramped up. The resulting change in the quadrupole strengths are shown in Fig. 4. In order to compensate for the additional vertical focusing of all 5 wigglers, QDH is decreased by about 1%, from -0.52684 to -0.5214. The focusing in the horizontal plane (due to a change in QDH) is corrected by decreasing QF by the same order of magnitude. The same parabolic dependence of the 'edge-focusing' force of the wiggler on field strength is reflected in these curves for the quadrupole settings.

Finally, we plot the modulations of the betatron function around the ring caused by the wigglers. Figures 5-8 indicate this change of $\frac{\beta_o - \beta_w}{\beta_o}$ (%). Beamlines #4 and #7 are located symmetrically on either side of the interaction points, resulting in an even or co-sinusoidal 10 period betatron perturbation ($\nu_y \sim 5.11$). This curve is used as a reference for the succeeding 3 plots. The largest excursion occurs at s=70m, which was estimated in Table 3 to be about 6.3%.

Adding beamline #5 results in the largest overall excursion (16%) as shown in Fig. 6. Table 3 estimates the linear perturbation of these first three beamline should reach almost 11% at s=70m. Note that the effect of adding beamline #6 (Fig. 7, Table 3) is to partially cancel the modulation induced by beamline #5. In fact, the two beamlines are separated by nearly $\frac{\pi}{4}$ in betatron phase. The distributed nature of the beamlines governs the overall detail in the beam envelope perturbation.

Finally, when beamline #10 is brought on line, the betatron modulation with all wigglers at full power is plotted in Fig. 8. The perturbations in the West side of SPEAR are 180° out of phase from and comparable in magnitude to the initial case with beamlines #4 and #7 active. The largest envelope modulations (up to 8%) still persist in the North- and South-East quadrants of the ring.

Conclusions

Calculations and numerical simulations of the linear tune shift and vertical betatron modulation generated by the 5 SSRL insertion devices in SPEAR show that these devices should not interfere stable beam operation. The tune shift with all wigglers active, however, is on the order of 0.04 and must be corrected to avoid crossing synchrobetatron resonances in SPEAR. To correct the tune shift, the strength of the quadrupoles QF and QDH in the FODO cells must be decreased by a total of about 1% as shown above.

It should be noted that non-linear effects have not been investigated in this memo. Further work is recommended in this area. In particular, tracking studies to assess the effect of non-linearities intrinsic to the wiggler magnets, assessment of closed orbit distortions, and investigations into the off-momentum behavior should be considered. In addition, the effect of the wigglers on the dynamic aperture may be important to beam lifetime. The lattice simulation code 'GEMINI' is ideally suited to applications in all of these areas.

Following the prescribed sequence for wiggler activation, namely, beamlines 4 and 7 (operated in parallel) followed by beamlines 5, 6 and10 with periodic tune corrections, the vertical betatron modulation can be maintained below 16%. In this case, the maximum increase in the vertical beam size relative to the case with no wigglers active is only about 8%. Although the effect on beam size (β) is not great, there is a noticeable effect on the photon beam spot-size at the radiation targets. The main challenge with insertions in SPEAR will be to maintain constant tunes during the dynamic processes of ramping and wiggler gap closure. Attempts to re-match the mini-beta HEP insertions to the arcs with the wigglers present led to unacceptable lattice configurations.

Acknowledgements

Many thanks to Hiroshi Nishmura and Etienne Forest of the ESG group at Berkeley for help using their 'GEMINI/FUTAGO' simulation package, and to Martin Donald for his insights into the complex nature of the beam optics and machine dynamics with wigglers in SPEAR. Max Cornacchia is responsible for initiating and coordinating this collaboration.

References

[1] 'Overview of Synchrotron Radiation Facilities', H. Winick, PAC Conf., March 20-23, Chicago, Ill., 1989. / Synchrotron Radiation', H. Winick, Bejing Symp.

on Appl. of Synch. Rad., May 27-June 7, 1988. / 'SSRL User Guide', P.O. Box 4349, Stanford, CA. 94309-0210, Bin 69.

[2] 'Vertically Integrated Simulation Tools for Self-Consistent Tracking and Analysis, E. Forest and H. Nishamura, PAC Conf., March 20-23, Chicago, Ill., 1989.

[3] 'The GEMINI-FUTAGO Model and Programs: A Summary', H. Nishamura and E. Forest, ESG Tech. Note-92, Sept. 1988

[4] 'Accelerator Physics', Course notes by H. Wiedemann, U.S. Particle Accelerator Summer School, UCB, June 19-30, 1989.

List of Figures

DISCLAIMER

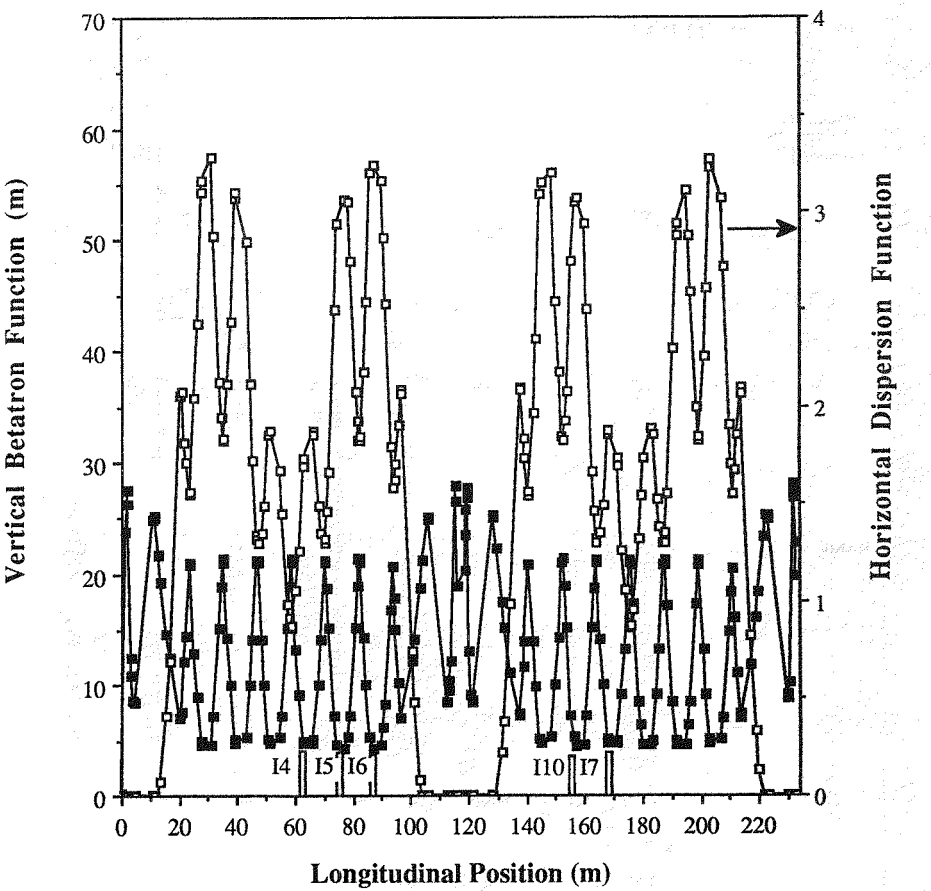

Fig. 1 Vertical betatron function and horizontal dispersion in SPEAR. Locations of SSRL insertion devices are indicated.

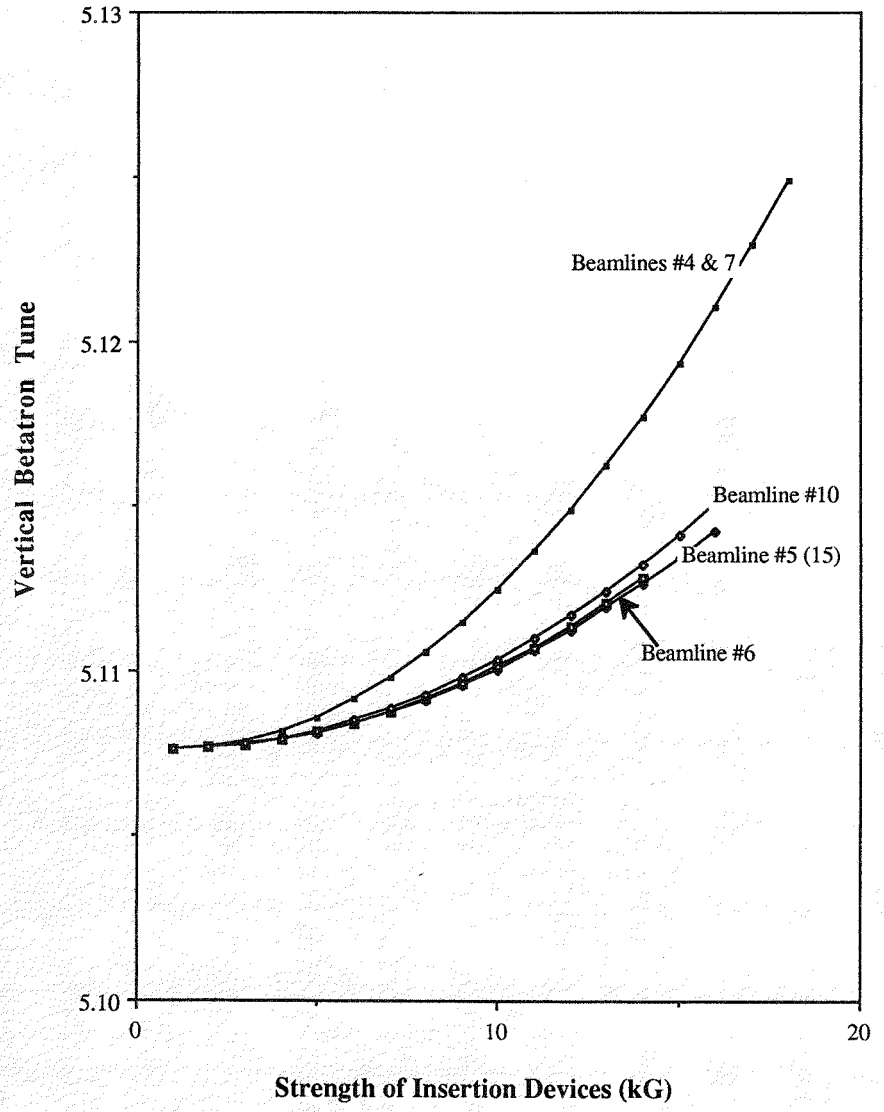

Fig. 2 Vertical tune shift induced by individual beamlines.

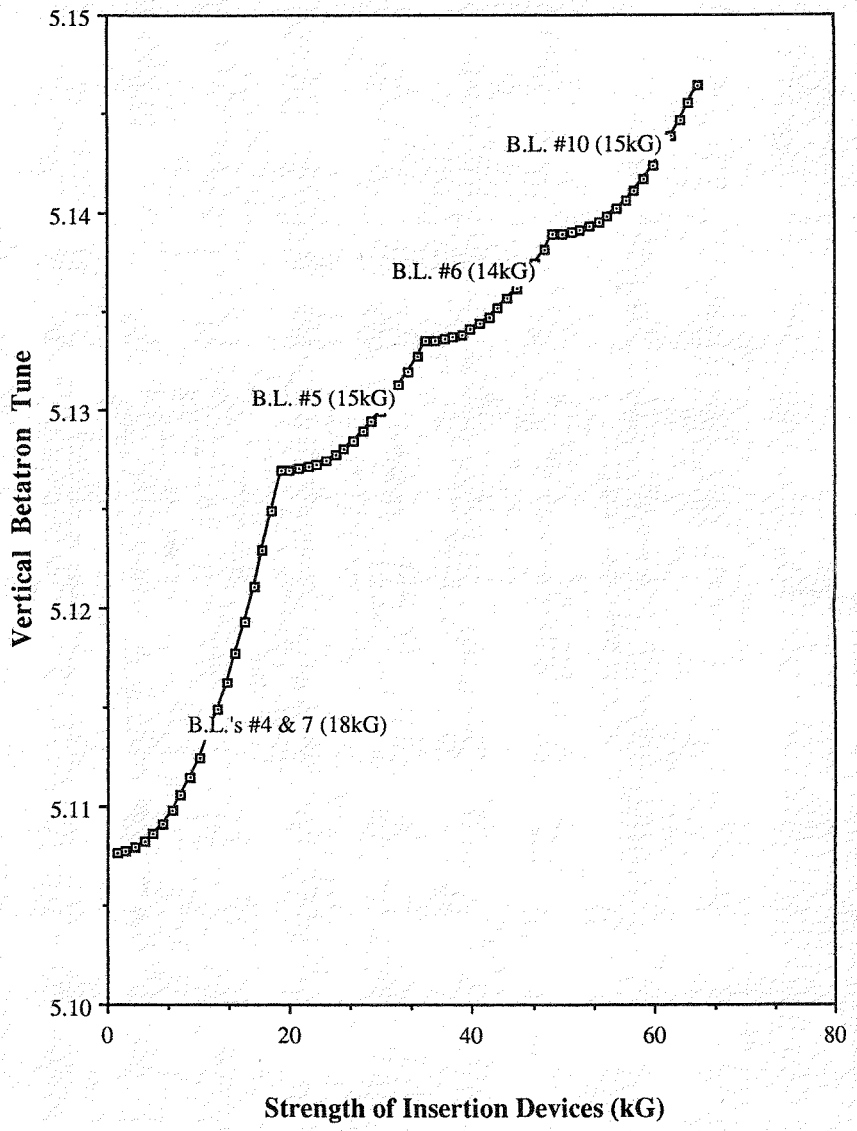

Fig. 3 Vertical tune shift with progressive beamline excitation.

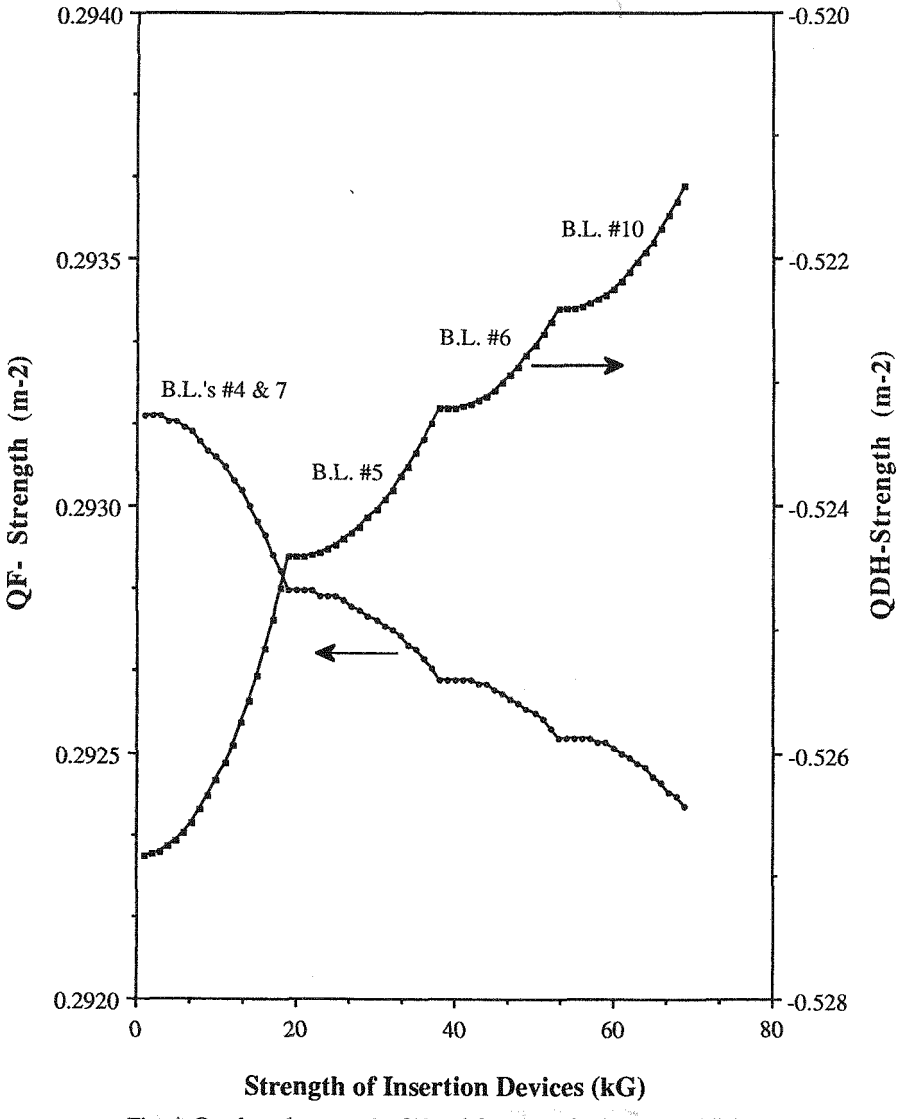

Fig. 4 Quadrupole strengths QF and QDH required to re-establish tunes.

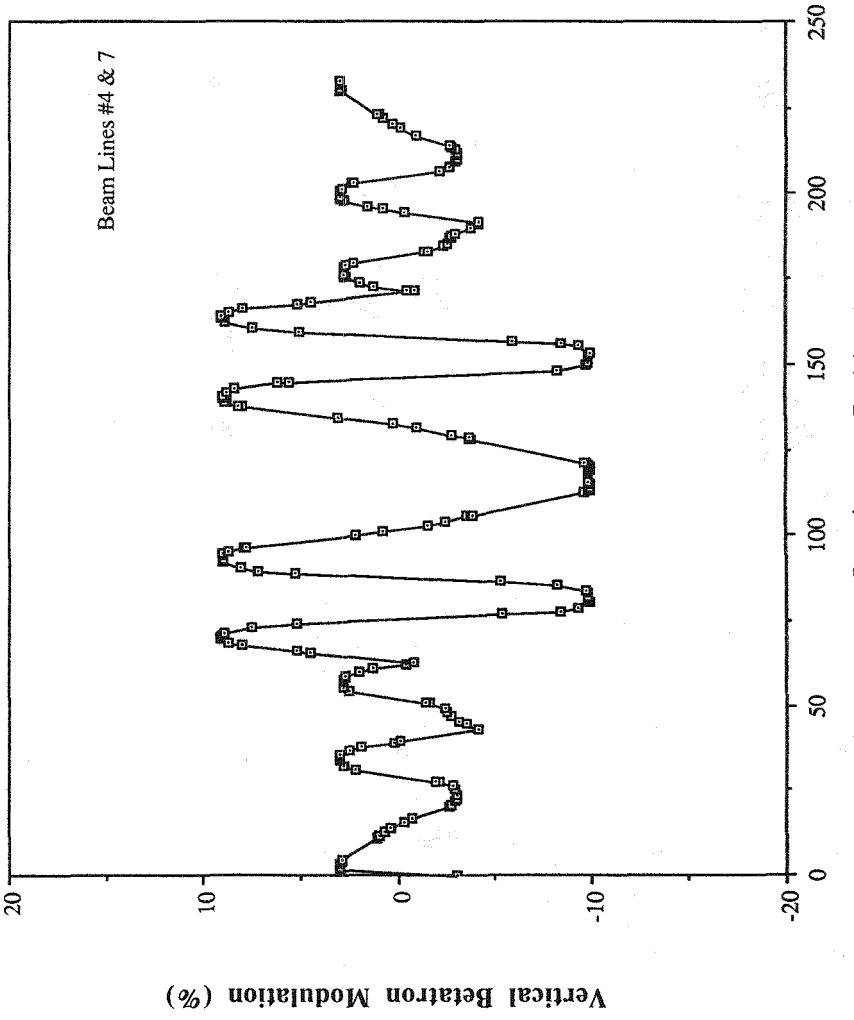

Fig. 5 Vertical betatron modulation induced by beamlines 4 + 7.

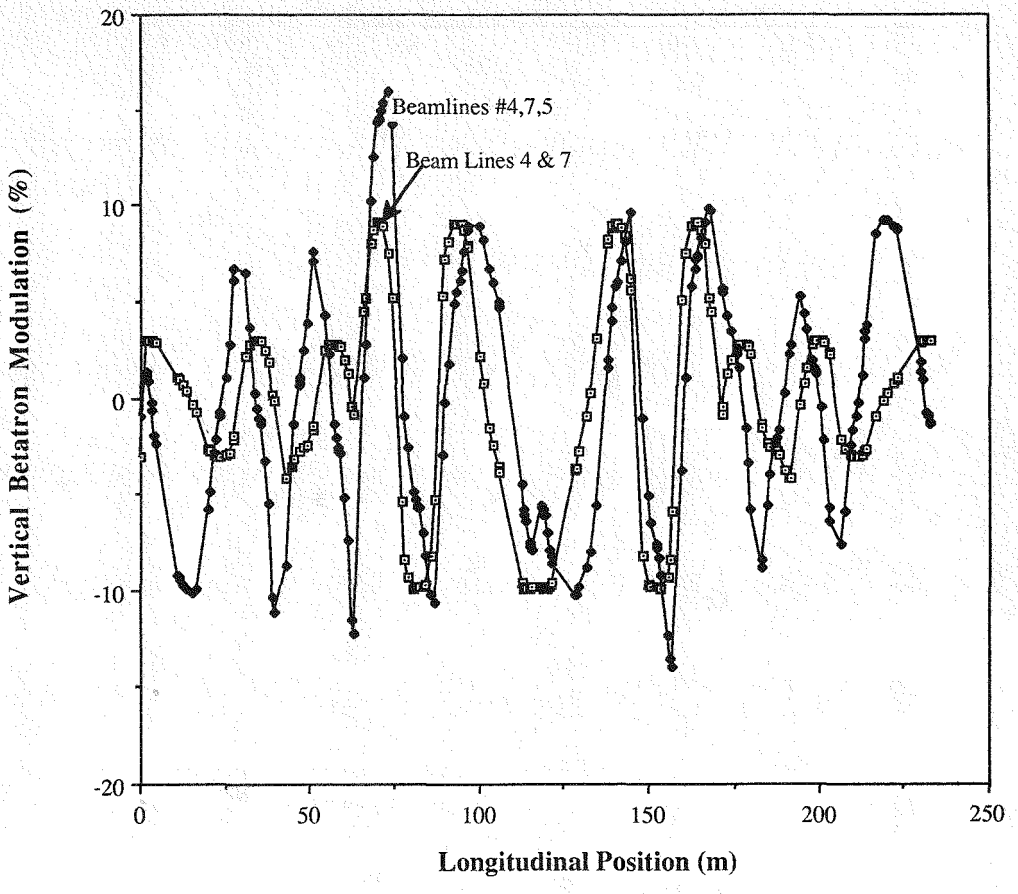

Fig. 6 Vertical betatron modulation induced by beamlines 4, 7, 5.

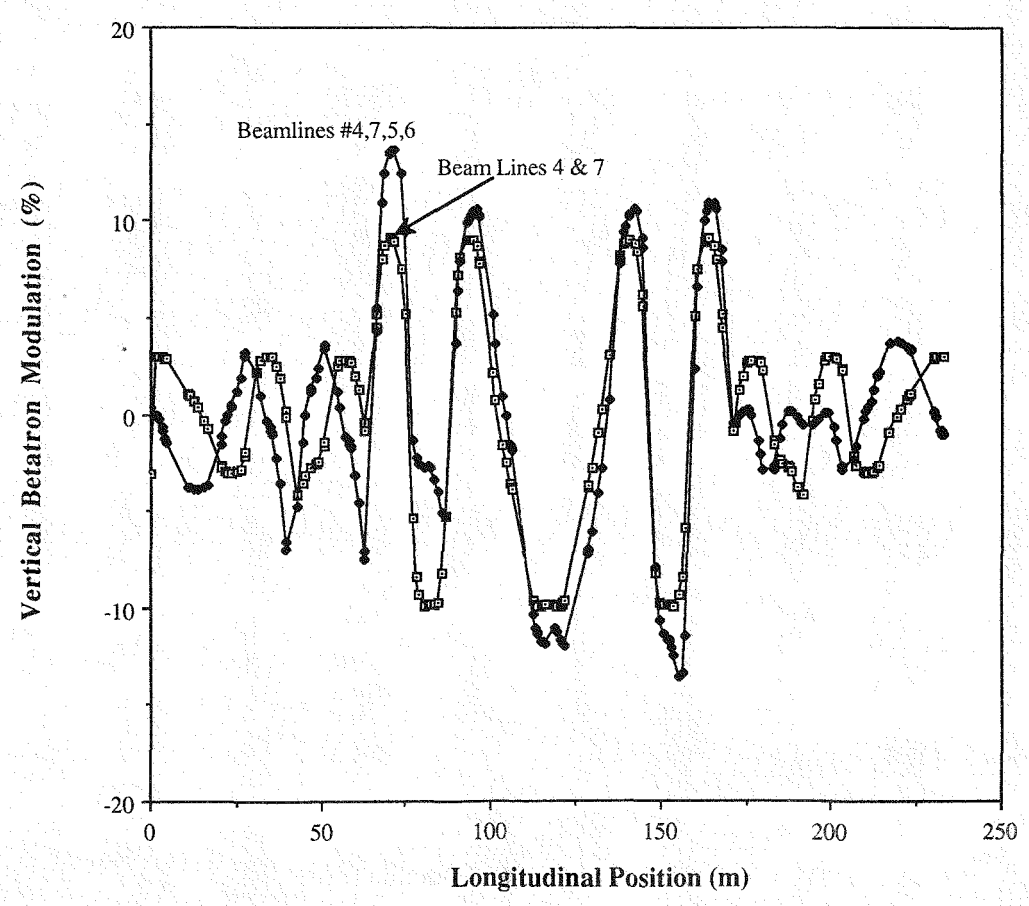

Fig. 7 Vertical betatron modulation induced by beamlines 4, 7, 5, 6.

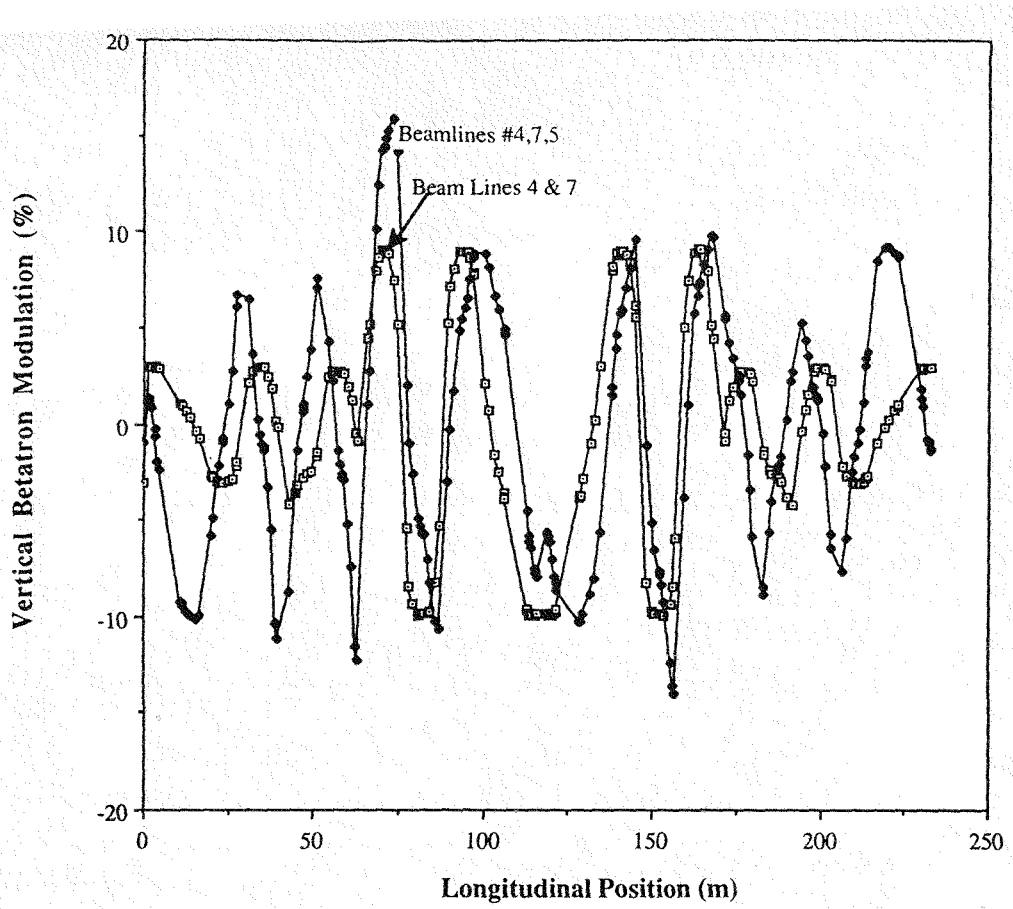

Fig. 6 Vertical betatron modulation induced by beamlines 4, 7, 5.

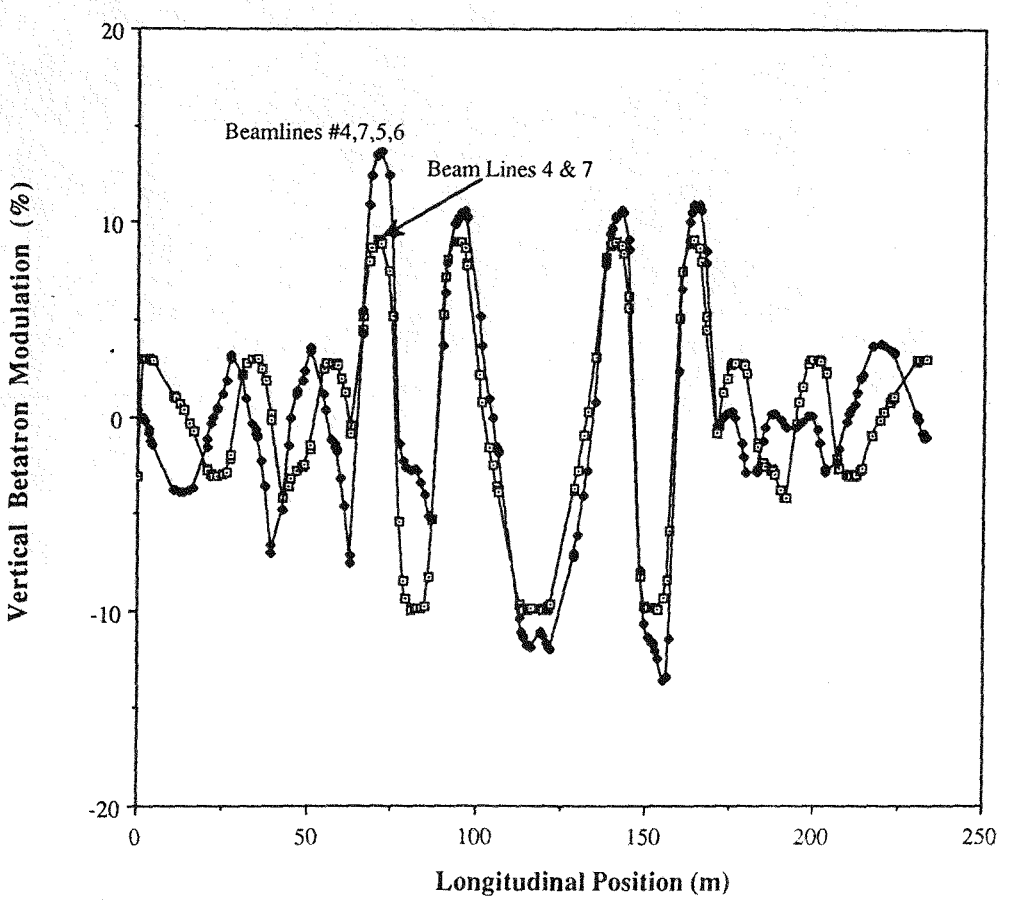

Fig. 7 Vertical betatron modulation induced by beamlines 4, 7, 5, 6.

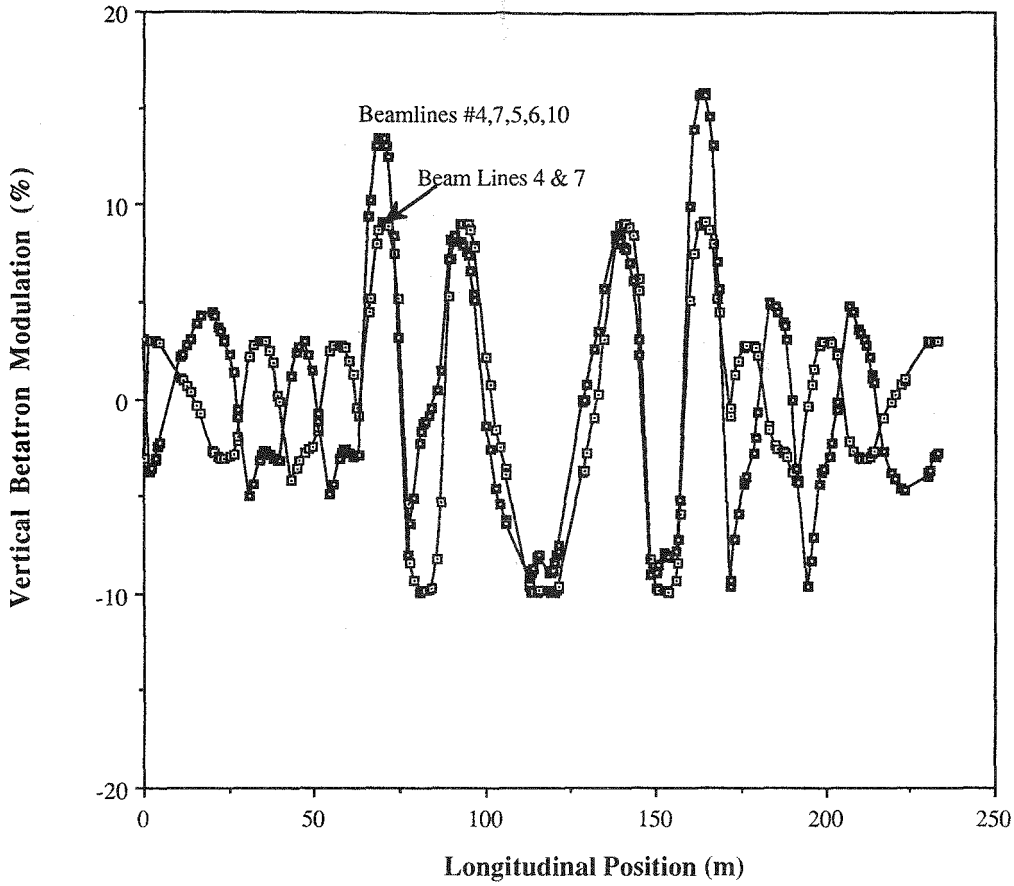

Fig. 8 Vertical betatron modulation induced by beamlines 4, 7, 5, 6, 10.